Available online at www.sciencedirect.com
SCIENCE DIRECT
Trans. Nonferrous Met. Soc. China 17(2007) 72−76
Transactions of Nonferrous Metals Society of China
www.csu.edu.cn/ysxb/

Effects of Ti addition on microstructures of melt-spun CuCr ribbons

WANG You-hong(王宥宏)[1,2], SONG Xiao-ping(宋晓平)[1], SUN Zhan-bo(孙占波)[1],
ZHOU Xuan(周 轩)[1], GUO Juan(郭 娟)[1]

1. School of Science, Xi'an Jiaotong University, Xi'an 710049, China;
2. Institute of Materials Science and Engineering, Taiyuan University of Science and Technology, Taiyuan 030024, China

Received 17 April 2006; accepted 27 August 2006

Abstract: The microstructure and resistivity of melt-spun CuCrTi ribbon were studied. The results reveal that the maximal size of the primary Cr particles in the microstructures is below 100 nm by 0.65%−3.8%Ti (mole fraction) addition and the resistivity of annealed ribbons of 0.65%−1.3%Ti addition can meet the need of the contact materials used by the medium-voltage vacuum interrupters. By contrasting the melt-spun microstructures to the annealed microstructures, the primary Cr particles do not grow up quickly in the annealing process. The X-ray diffraction studies reveal that alloying increases the amount of the solute in Cu and Cr phases and results in the increase of resistivity. By the thermodynamic analysis, adding Ti to $CuCr_{29}$ alloys increases the critical supercooling of the liquid/solid transformation, which makes the critical radius of nucleation decrease and the rate of nucleation increase. As a result, the microstructure of CuCr ribbon can be further refined.

Key words: CuCr alloys; melt spinning; thermodynamic; contact; resistivity

1 Introduction

The contact material based on CuCr alloys containing 20%−50% Cr has been widely investigated because it is a dominating contact material used in medium-voltage vacuum interrupters. It is an important subject to refine the Cr particles in its microstructure [1−2]. To improve its microstructure, many special preparation processes, such as powder sintering[2−3], molten metal infiltrating[4−5], self-consuming electrode [6], arc-melting[7] and low-segregation molten-casting [8] have been used. However the best refining result of Cr phase is still in micron-scale. The solubility of Cr in Cu in solid is so low that nearly no available heat treatment can be used to improve its microstructure. By the mechanical alloying, the CuCr alloys with nano Cr particles were recently obtained, and the sample has some excellent electric properties[9−11]. But the lower productivity and higher residual gas made it impossible to be applied widely.

Melt spinning is the most common method of rapid solidification nowadays. It is capable of refining the microstructure, extending the solid solubility limits and forming the metastable phase, etc. A number of studies[12−18] have been undertaken to investigate the microstructures of rapidly solidified metals. However, it has not been well used in the research of refining the microstructure of CuCr alloys.

The effect of Ti addition on the melt-spun microstructure of CuCr ribbon was based on the transmission electron microscopy investigation. Moreover, the change of the resistivity of alloying ribbon is paid a special attention because it is an important property of contacts.

2 Experimental

High-purity (>99.95%) Cu, Cr and Ti were used to prepare the CuCrTi alloys. The material was arc-melted employing a non-consumable tungsten electrode. Subsequently, the material with a mass of 10 g was inserted into a quartz tube. When the material was heated by high frequency induction to the required temperature, the ribbon was prepared by liquid quenching on a single roller melt spinning under a pressure of 50.5 kPa Ar gas. The velocity of the cooling roller was 33 m/s, the calculated cooling rate of ribbon was about 10^6 K/s

Foundation item: Project(50371066) supported by the National Natural Science Foundation of China
Corresponding author: WANG You-hong; Tel: +86-351-6999329; E-mail: Wyheyj@163.com

according to our work[19]. The dimensions of prepared ribbons were about 3 mm in width and 25−40 μm in thickness. Under this condition, the maximal undercooling of ribbon is about 400−450 K[13,17].

Some melt-spun ribbon was annealed in a vacuum furnace at 600 ℃ for 2−16 h. The microstructure was studied by a Hitachi H-800 transmission electron microscope(TEM). The foil specimen for TEM was prepared by a twin-jet thinning device. The lattice parameters of the Cu and Cr phases in the melt-spun and annealed ribbons were analyzed by a Rigaku D/max 2400 X-ray diffractometer(XRD). The resistivity of ribbon was measured by the four point probe method.

3 Results

The microstructure of melt-spun $CuCr_{29}$ ribbon is shown in Fig.1. The spherical particle marked by an arrow is a primary Cr particle. The diameter of the primary Cr particle is about 200 nm. Using melt spinning, the size of the primary Cr particle in the CuCr microstructure can be refined from the micron-scale to nano-scale, which reveals that the microstructure of CuCr alloys can be markedly refined by increasing cooling rate of solidification process. The performance of CuCr contact is mainly affected by the primary Cr particles in its microstructure[1−11]. The resistivity of annealed $CuCr_{29}$ ribbons is about 4.53 μΩ·cm as shown in Table 1.

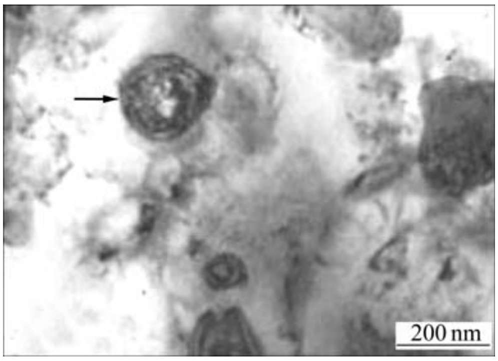

Fig.1 Microstructure of melt-spun $CuCr_{29}$ ribbon (Arrow notes primary Cr particle)

3.1 $CuCr_{28.8}Ti_{0.65}$ alloys

Fig.2(a) shows the microstructure of melt-spun $CuCr_{28.8}Ti_{0.65}$ ribbon. The diameter of the primary Cr particle marked by an arrow is below 100 nm. When the ribbon is annealed at 600 ℃ for 2 h, the diameter of the primary Cr particle marked by an arrow in Fig.2(b) is also below 100 nm. The result means that the addition of Ti to CuCr alloys can preferably refine their melt-spun microstructure and the microstructure of melt-spun $CuCr_{28.8}Ti_{0.65}$ alloys will not transform obviously in the latter process. The change of the precipitates in microstructure is not conspicuous. The X-ray diffraction study, as shown in Fig.3, reveals that the lattice parameters of melt-spun and annealed Cu matrix and Cr phase are increased by Ti addition, seen in Table 1. This means that alloying increases the amount of the solute in Cu and Cr phases, which results in the fact that the

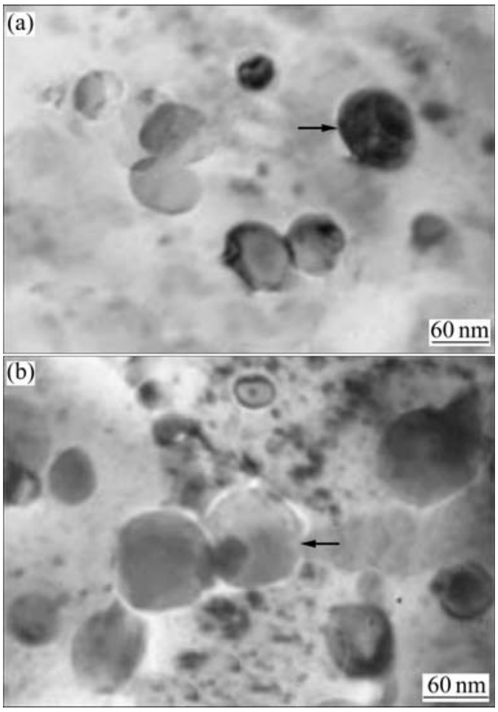

Fig.2 Microstructures of melt-spun $CuCr_{28.8}Ti_{0.65}$ ribbons (Arrows respectively note primary Cr particles): (a) Melt-spun; (b) Annealed at 600 ℃ for 2 h

Table 1 Lattice parameters and resistivities of melt-spun CuCrTi ribbon

Mole fraction/%			Lattice parameter/Å				Resistivity/(μΩ·cm)	
			FCC Cu phase		BCC Cr phase			
Cu	Cr	Ti	Melt-spun	Annealed	Melt-spun	Annealed	Melt-spun	Annealed
71.0	29	−	3.617 7	3.611 6	2.881 7	2.879 3	12.77	4.53
69.8	28.8	0.65	3.617 9	3.617 2$^{1)}$	2.884 2	2.883 1$^{1)}$	14.15	5.03
68.9	28.6	1.3	3.618 2	3.617 9$^{2)}$	2.886 9	2.883 5$^{2)}$	16.78	6.12
68.4	27.8	3.8	3.619 5	3.618 2$^{3)}$	2.887 8	2.885 2$^{3)}$	25.29	11.27

1) Annealed at 600 ℃ for 2 h; 2) Annealed at 600 ℃ for 5 h; 3) Annealed at 600 ℃ for 16 h

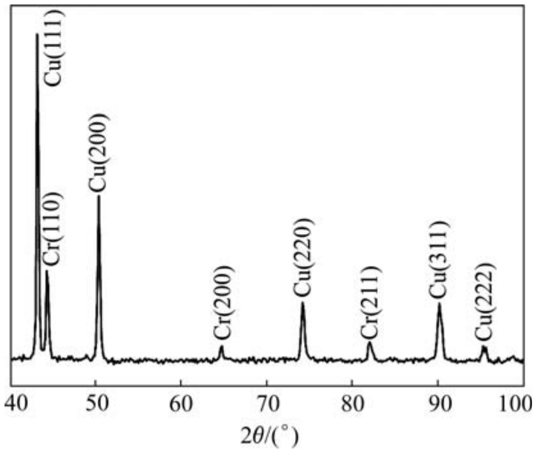

Fig.3 X-ray pattern of melt-spun $CuCr_{28.8}Ti_{0.65}$ ribbons

resistivity of annealed $CuCr_{28.8}Ti_{0.65}$ ribbon is increased to 5.03 μΩ·cm. This value is a little higher than that of $CuCr_{29}$ ribbons, as shown in Table 1. From Fig.3 and Table 1, it can be seen that Ti element is dissolved in Cu matrix and Cr phase.

3.2 $CuCr_{28.6}Ti_{1.3}$ alloys

The microstructures of melt-spun $CuCr_{28.6}Ti_{1.3}$ ribbon are shown in Fig.4. Most of primary Cr particles in the microstructure in Fig.4(a) are refined to less than 80 nm. When the ribbon is annealed at 600 ℃ for 5 h, the Cr particles in Fig.4(b) do not grow up much. The X-ray diffraction pattern reveals that the lattice parameters of melt-spun and annealed Cu matrix and Cr phase are continuously increased with the increase of Ti content, as shown in Table 1. Its X-ray pattern is similar to Fig.3. The resistivity of annealed $CuCr_{28.6}Ti_{1.3}$ ribbons is about 6.12 μΩ·cm.

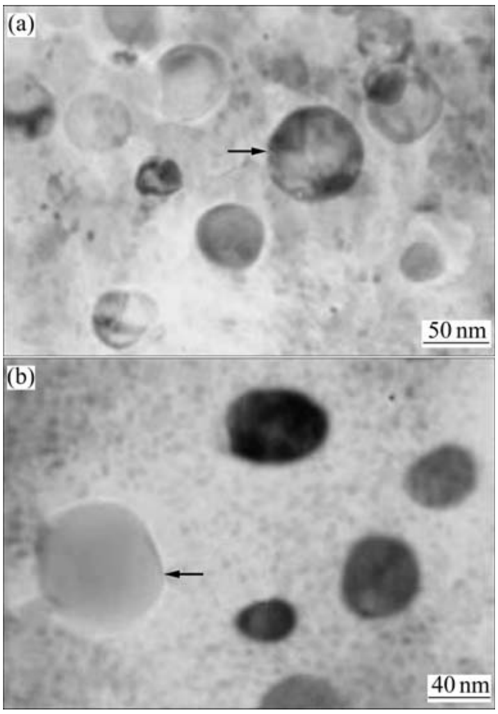

Fig.4 Microstructures of melt-spun $CuCr_{28.6}Ti_{1.3}$ ribbons (Arrows respectively note primary Cr particles): (a) Melt-spun; (b) Annealed at 600 ℃ for 5 h

3.3 $CuCr_{27.8}Ti_{3.8}$ alloys

The microstructures of melt-spun and annealed $CuCr_{27.8}Ti_{3.8}$ ribbons in Fig.5 are further refined. The maximal diameter of the primary Cr particles in the melt-spun and annealed microstructures is smaller than 50 nm. However, the resistivity of annealed $CuCr_{27.8}Ti_{3.8}$ ribbon is increased to 11.27 μΩ·cm, which may be too high to be used by the medium-voltage vacuum interrupters (There is no resistivity standard for the contact materials in the world).

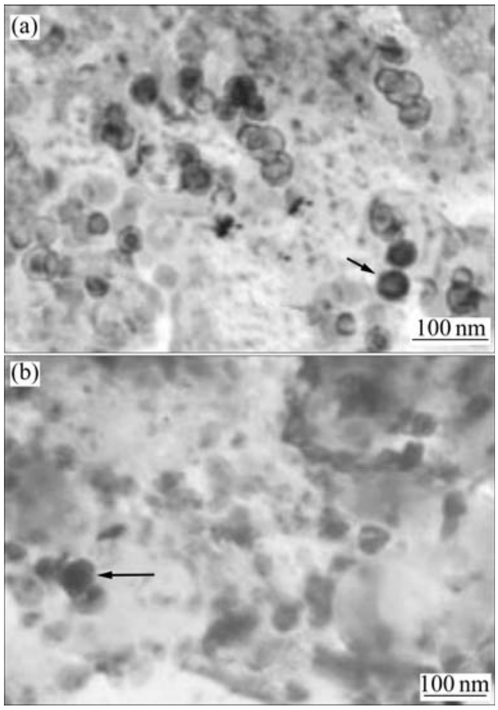

Fig.5 Microstructures of melt-spun $CuCr_{27.8}Ti_{3.8}$ ribbons (Arrows respectively note primary Cr particle): (a) Melt-spun; (b) Annealed at 600 ℃ for 16 h

4 Discussion

The reason of melt spinning to refine the microstructure is based on its very high cooling rate, which has been studied in Refs.[12−18]. The effect of Ti addition on the microstructure of CuCr alloys will be discussed below by thermodynamics.

According to regular solution model, the mixing Gibbs free energy (G_m) of multi-component alloy system can be expressed as

$$G_m = RT\sum_{i=1}^{n} x_i \ln x_i + \sum_{i=1}^{n}\sum_{j=i+1}^{n} \Omega_{ij} x_i x_j \tag{1}$$

where x_i and x_j are the molar fraction of components i

and j; Ω_{ij} is the interaction parameters between components i and j; R is the gas constant (8.31 J/(mol·K)), T is temperature in K.

Using the published data in Refs.[20−22], the mixing Gibbs free energies of the liquid phases and the BCC Cr solid phases in CuCr and CuCrTi systems at 1 500 K were calculated by Eqn.(1). Moreover, the mixing Gibbs free energy differences (ΔG_{mx}) between homogeneous liquids and the separated liquids in these systems were also calculated. The result is shown in Fig.6. It is revealed by the calculation that Ti addition can obviously decrease the G_m and ΔG_{mx} of CuCr liquid, however, the G_m of BCC Cr phase is decreased a little. The critical temperature of the liquid phase separation [20] to CuCr system is about 1 500 K. The primary Cr particles in the melt-spun and annealed microstructures are not from general solidification process, but are formed in the liquid phase separation process. The liquid phase separation is bad to refine the microstructure of alloys.

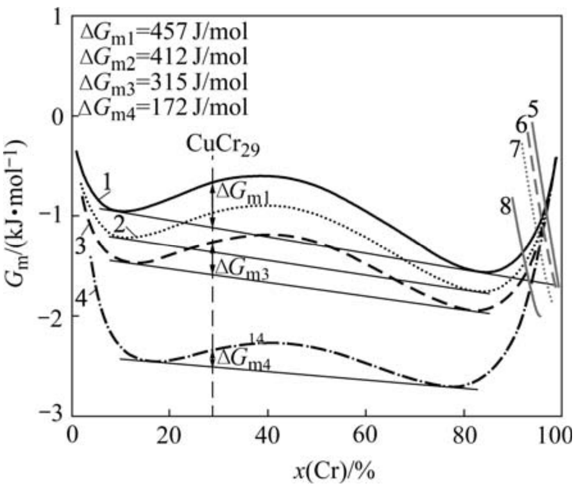

Fig.6 Effects of adding Ti on mixing Gibbs free energy (in liquid and Cr solid) and difference of mixing Gibbs free energy in liquid (ΔG_{mx}) of Cu-Cr system at 1 500 K: 1 L-CuCr; 2 L-CuCr$Ti_{0.65}$; 3 L-CuCr$Ti_{1.3}$; 4 L-CuCr$Ti_{3.9}$; 5 Cr_{BCC}-CuCr; 6 Cr_{BCC}-CuCr$Ti_{0.65}$; 7 Cr_{BCC}-CuCr$Ti_{1.3}$; 8 Cr_{BCC}-CuCr$Ti_{3.9}$

The decrease of G_m in liquid results in the phenomenon that the liquid phase separation will occur at lower temperatures and the reduction of ΔG_{mx} will decrease the driving forces of liquid phase separation. They will make the liquid phase separation process be restrained.

Adding Ti to CuCr alloys, the decrease of G_m in liquid will make the undercooling liquid more steady and the beginning temperature of the liquid/solid transformation lower. The difference between liquidus and the actual temperature of undercooling liquid is enlarged, so the actual undercooling (ΔT) of liquid should be increased.

According to the solidification theory[23], we know that the critical radius of nucleation (r^*) is

$$r^* = -\frac{2\sigma T_m V_s}{\Delta H \Delta T} \tag{2}$$

where σ is the surface energy; T_m is the liquidus; V_s is the mole volume; ΔH is the difference of enthalpy between liquid and solid; ΔT is the critical supercooling.

By the Eqn.(2), r^* will be decreased as ΔT increases, which results in the increase of the number of nucleus and the refinement of microstructure.

On the other hand, the rate of nucleation (I)[23] is

$$I = B_1 \frac{D_L}{D_{LM}} \exp\left[-\frac{16\pi\sigma^3 T_m^2 V_s^2}{3\Delta H^2 \Delta T^2 kT}\right] \tag{3}$$

where B_1 is a coefficient that is decided by the critical radius of nucleation and the surface energy; D_L is the diffusivity in liquid; D_{LM} is the diffusivity in liquid at melting point; k is Boltzmann constant; T is the temperature of supercooling liquid.

By Eqn.(3), the relation between I and ΔT satisfies or meets the Gaussian distribution. For melt spinning, as ΔT increases, I will be increased, and the microstructure will be refined.

5 Conclusions

1) Using melt spinning, the size of the primary Cr particles in the CuCr microstructure can be refined from the micron-scale to about 200 nm, which reveals that with the increase of the cooling rate of solidification process, the microstructure of CuCr alloys can be markedly refined.

2) The primary Cr particles in the microstructures of $CuCr_{29}$ ribbon can be refined to less than 100 nm by 0.65%−1.3% Ti addition and its resistivity is not increased much. Adding 3.8%Ti to $CuCr_{29}$ alloys, the primary Cr particles in its microstructures can be refined to less than 80 nm, but the resistivity of its ribbon will be obviously increased. By contrasting the melt-spun microstructures to the annealed microstructures, the primary Cr particles do not grow up quickly in anneal process.

3) The X-ray diffraction pattern reveals that Ti addition increases the lattice parameters of melt-spun and annealed Cu matrix and Cr phase, which means that alloying increases the amount of the solute in Cu and Cr phases and results in the increase of resistivity.

4) By the thermodynamic analysis, it reveals that adding Ti to CuCr alloys can obviously decrease the G_m of liquid. As a result, the critical undercooling of the liquid/solid transformation is increased, which makes the critical radius of nucleation decrease and the rate of

nucleation increase, and the microstructure of CuCr ribbon can be further refined.

References

[1] RIEDER W F, SCHUSSEK M, GLATZLE W, KNY E. The influence of composition and Cr particle size of Cu/Cr contacts on chopping current, contact resistances and breakdown voltage in vacuum interrupters [J]. IEEE Trans CHMT, 1989, 12(2): 273−278.

[2] WANG Y, DING B. The preparation and the properties of microcrystalline and nanocrystalline CuCr contact materials [J]. IEEE Trans CPMT, 1999, 22(2): 467−472.

[3] DING B, YANG Z, WANG X. Influence of microstructure on dielectric strength of CuCr contact materials in a vacuum [J]. IEEE Trans CPMT, 1996, 19(1): 76−81.

[4] SPAIC S, KOMAC M, FETAHAGIC A. Microstructure and properties of sintered Cu-25Cr alloy [J]. Materials Science and Technology, 1989, 5(11): 1069−1073.

[5] DING B J. Control of Composition, Microstructure of Contact Materials for Vacuum Interrupts and Their Effects on Electrical Prosperities [D]. Xi’an: Xi’an Jiaotong University, 1990. (in Chinese)

[6] YANG Z M. Influence of Alloying Elements and Microstructures on Dielectric Strengths, Interrupting Abilities and Chopping Currents of Vacuum Contact Materials [D]. Xi’an: Xi’an Jiaotong University, 1996. (in Chinese)

[7] XIU S X, ZOU J Y, HE J J. Influence of microcosmic characteristic of CuCr contact materials on their macroscopical properties [J]. High-Votage Electr Equip, 2000, 36(3): 40−43.

[8] ZHAO F, YANG Z M, DING B J. Preparation of CuCr25 alloys through vacuum arc-smelting and their properties [J]. Trans Nonferrous Met Soc China, 2000, 10(1): 73−75.

[9] CAO H, XIAN A P. The deformation and refining of structure of CuCr25 alloy [J]. Chin J Nonferrous Met, 2002, 12: 570−574.

[10] FENG Yu, ZHANG Cheng-yu, DING Bing-jun. Preparation of nanocrystalline CuCr contact materials and their chopping currents [J]. Rare Metal Materials and Engineering, 2005, 34(9): 1439−1442.

[11] CAO Hu, WANG Ya-ping, ZHENG Zhi, XIAN Ai-ping. Properties of CuCr contact materials with low chromium content and fine particle [J]. Trans Nonferrous Met Soc China, 2003, 13(4): 930−932.

[12] ZHANG Zhong-hua, BIAN Xiu-fang, WANG Yan, LIU Xiang-fa. Microstructures and modification performance of melt-spun Al-10Sr alloy [J]. Journal of Materials Science, 2002, 37: 4473−4480.

[13] MASLOV V V, NOSENKO V K. Microstructure formation processes in melt spun and bulk undercooled Fe- and Ni-base alloys [J]. Journal of Materials Science, 2002, 37: 4663−4668.

[14] TIANYI C, LÖSER W, LEONHARDT M. Effects of composition on microstructures of rapidly solidified Ni-Al alloys [J]. Journal of Materials Science, 1998, 33: 4365−4374.

[15] ZHANG Lin, WU You-shi, BIAN Xiu-fang, XING Zhi-na. Effects of quenching rate on the microstructure of a rapidly solidified Zn-5wt%Al alloy [J]. Journal of Materials Science, 1999, 18: 1969−1972.

[16] NAGARAJAN R, MANJINI S, CHATTOPADHYAY K, AOKI K. The effect of ternary addition of silicon on the structure and microstructure of rapidly solidified equiatomic TiNi alloys [J]. Journal of Materials Science, 1997, 32: 6021−6027.

[17] LIU Feng, YANG Gen-cang, GUO Xue-feng. Comparison of microstructure and solidification behavior of rapid quenching with bulk undercooled superalloy [J]. Journal of Materials Science, 2001, 36: 3607−3615.

[18] COOPER K P, JONES H N. Microstructural evolution in rapidly solidified Al-Cu-Si ternary alloys [J]. Journal of Materials Science, 2001, 36: 5315−5323.

[19] WANG You-hong, SUN Zhan-bo, SONG Xiao-ping. Numerical simulation of single roller melt-spinning for solidification process of Cu-Cr alloy [J]. The Chinese Journal of Nonferrous Metals, 2005, 15(7): 1045−1049.(in Chinese)

[20] THOMAS J K, SHASHANK P, WASEDA Y. A thermodynamic study of liquid Cu-Cr alloys and metastable liquid immiscibility [J]. Z Metallkd, 2000, 91(7): 594−600.

[21] PAN Wei, LIAN Jie. Thermodynamics of Ti in Cu-Ti alloy investigated by the EMF method [J]. Mater Sci Eng, 1999, A269: 104−110.

[22] LEE J Y, KIM J H, PARK S, et al. Phase equilibrium of the Ti-Cr-V ternary system in the non-burning b-Ti alloy region [J]. J All Comp, 1999, 291: 229−238.

[23] FLEMINGS M C. Solidification Processing [M]. USA: McGraw-Hill, Inc, 1974: 303−304.

(Edited by LI Xiang-qun)